

Minimization of turning time for high-strength steel with a given surface roughness using the Edgeworth–Pareto optimization method

A. T. Abbas¹ · D. Yu. Pimenov² · I. N. Erdakov³ · T. Mikolajczyk⁴ · E. A. El Danaf¹ · M. A. Taha⁵

Received: 7 April 2017 / Accepted: 14 June 2017 / Published online: 1 July 2017
© The Author(s) 2017. This article is an open access publication

Abstract High-strength steels are used in various civilian and military products. The initial cost of the raw materials for these products is very high. The surface roughness of these products is extremely important during the finishing pass to be accepted during the final inspection. The surface roughness should conform to the required values stated on the design drawing. The paper presents the results of experiments in turning of high-strength steel featuring three factors—cutting speed V , feed rate

f , and depth of cut t —on five levels (125 specimens). These were divided into 25 groups. Each of the five groups was subjected to one common machining speed. Each group was machined using five levels of cutting depth. Each depth was processed using five levels of feed rate. Tessa was used for examination of surface roughness. There is little modern research on machining high-strength steel. The high cost of this material compels us to look for the optimum turning conditions to provide for the specified roughness of surface Ra and the minimum machining time of unit volume T_m . As a result of our study, an artificial neural network was designed in Matlab on the basis of the MLP 3-10-1 multilayer perceptron that allows us to predict Ra of the workpiece with $\pm 2.14\%$ accuracy within the range of the experimental cutting speed, depth of cut, and feed rate values. For the first time, a Pareto frontier was obtained for Ra and T_m of the finished workpiece from high-strength steel using the artificial neural network model that was later used to determine the optimum cutting conditions. It is possible to integrate the suggested optimization algorithms into computer-aided manufacturing using Matlab.

✉ D. Yu. Pimenov
danil_u@rambler.ru

A. T. Abbas
atabbas1954@yahoo.com

I. N. Erdakov
wissenschaftler@bk.ru

T. Mikolajczyk
tami@utp.edu.pl

E. A. El Danaf
edanaf@ksu.edu.sa

M. A. Taha
eng_mohamed_2017@yahoo.com

Keywords Artificial neural network · High-strength steel · Turning operation · Optimization · Edgeworth–Pareto method · Surface roughness · Data mining

¹ Department of Mechanical Engineering, College of Engineering, King Saud University, Riyadh 11421, Saudi Arabia

² Department of Automated Mechanical Engineering, South Ural State University, Lenin Prosp. 76, Chelyabinsk 454080, Russia

³ Department of Pyrometallurgical and Casting Technologies, South Ural State University, Lenin Prosp. 76, Chelyabinsk 454080, Russia

⁴ Department of Production Engineering, UTP University of Science and Technology, Al. prof. S. Kaliskiego 7, 85-796 Bydgoszcz, Poland

⁵ Department of Mechanical Design and Production, Faculty of Engineering, Zagazig University, Zagazig 44519, Egypt

Nomenclature

d	Diameter of cut (mm)
l	Length of parts (mm)
α	Back angle ($^{\circ}$)
k_r	Cutting edge angle ($^{\circ}$)
r_o	Nose radius (mm)
V	Cutting speed (m/min)
t	Depth of cut (mm)
f_z	Feed rate (mm/rev)

DM	Decision maker
M	number of criteria
$I = \{1, 2, \dots, m\}$	A set of criteria numbers
X	A set of possible decisions
$f = (f_1, f_2, \dots, f_m)$	Vector-valued criterion
$Y = f(X)$	A set of possible vectors (estimates)
R_m	Euclidean space of m -dimensional vectors with real components
$\succ X$	Preference relation of DM specified in the set X
$\succ Y$	Preference relation of DM, induced on the set with $\succ X$ ratio and specified in the set Y
\succ	Relation $\succ Y$ continued in the entire space R_m
$\succ \text{Sel}X$	A set of selected decisions
$\text{Sel}Y$	A set of selected vectors (estimates)
$N\text{dom}X$	A set of non-dominated decisions
$N\text{dom}Y$	A set of non-dominated vectors (estimates)
$P_f(X)$	A set of Pareto optimal decisions
$P(Y)$	A set of Pareto optimal vectors (Pareto optimal estimates)
$f_1(Ra)$	Surface roughness (μm)
$f_2(Tm)$	Machining time of unit volume in one cutting tool pass (min/cm^3)
Ra_i	Surface roughness for current V, t and f_z parameter combinations (μm)
Ra_{max}	Maximum surface roughness value of all the V, t and f_z combinations (μm)
Tm_i	Machining time of unit volume for current V, t and f_z parameter combinations (min/cm^3)
Tm_{max}	Maximum machining time of unit volume value of all the V, t and f_z combinations (min/cm^3)

1 Introduction

Turning is commonly used to produce parts in many industries, such as machinery, automobiles, and machine tools. One of the main indicators of the surface quality of finish turning is surface roughness. High-strength steels are used in the production of high-pressure vessels that require ultra-precision turning. Examples of these high-pressure products include gun barrels, food sterilization equipment, high-precision sintering dies, hypersonic (up to Mach 16) wind tunnels, water jet cutting nozzles, and turbine casings for efficient power generation. Due to the limited resources in the modern world, efficient and rational utilization of resources stands out as an urgent task. Thus, developing resource-saving

technologies, including for turning operations, is a crucial point of interest. In the case of machining essential components fabricated from high-strength steel, minimizing the surface roughness Ra and maximizing the machining time of unit volume is a very important task to ensure the production of products with better surface quality using the minimum resources. In anticipation of the next sixth technology revolution, it is becoming an increasingly important technique for processing large data sets using artificial intelligence and the integration of artificial intelligence algorithms in automated production.

Many previous investigations have been devoted towards developing prediction models for rough turning [1–19]. Risbood et al. [1] researched and produced models for forecasting roughness and dimensional deviation for dry and wet turning of mild steel rods. Bajić et al. [2] investigated the effect of cutting speed, feed rate, and depth of cut on the surface roughness and cutting force components in longitudinal turning. For the model predictions of surface roughness, regression analysis and neural networks were used. Muthukrishnan and Davim [3] analyzed the turning of Al/SiC-MMC using ANOVA and artificial neural networking (ANN) to develop prediction models of surface roughness. In a study by Ali and Dhar [4] and with the help of artificial neural networks, a prediction model of surface roughness and tool wear was derived. Pontes et al. [5] provided an overview on the use of artificial neural networks to simulate the surface roughness for various types of machining. Natarajan et al. [6] reported the turning of brass C26000 material and the deduced prediction model of surface roughness using artificial neural network (ANN) based on Matlab. Svalina et al. [7] analyzed the effect of the depth of cut, feed rate, and speed on the surface roughness, which is predicted by using neural networks. Abdullah et al. [8] reported a model for predicting surface roughness obtained by turning AISI 4140 steel using ANN and the Taguchi method. Pontes et al. [9] presented a study on the applicability of the radial basis function (RBF) neural networks to predict surface roughness (Ra) in the process of turning SAE 52100 hardened steel, using orthogonal arrays, where Taguchi was implemented as a tool for the development of the network parameters. Asiltürk [10] proposed a model with a standard error of 0.002917120% for predicting the surface roughness of AISI 1040 steel material using artificial neural networks (ANN) and multiple regression model (MRM). Upadhyay et al. [11] used vibration signals to predict surface roughness during turning of Ti-6Al-4 V by applying multiple regression and an artificial neural network model. Ahilan et al. [12] developed a model predicting power consumption and

surface roughness when turning workpieces of AISI 304. Azam et al. [13] investigated the relationship of average surface roughness and processing parameters (feed, speed and depth of cut) for turning high-strength low-alloy steel (AISI 4340). Acayaba and Escalona [14] developed a model for predicting surface roughness in low speed turning of AISI316 austenitic stainless steel using multiple linear regression and artificial neural network techniques. Al Bahkali et al. [15] studied the effect of feed, cutting depth, radius of curvature of the tool tip and the cutting speed on surface roughness in turning cast iron. Mia and Dhar [16] developed an artificial neural network (ANN) model to predict the average surface roughness in turning hardened steel EN 24 T. Jurkovic et al. [17] compared three machine learning methods for predicting the high-speed turning observed parameters (surface roughness (Ra), cutting force (F_c), and the tool life (T)). Tootooni et al. [18] reported surface roughness using a non-contact measurement method during the turning process. Abbas [19] analyzed the effect of the feed rate, depth of cut and cutting speed on the surface roughness in turning high-strength steel. Though all the previously mentioned research [1–19] provided prediction models of surface roughness, they failed to solve the problem of determining the optimal cutting parameters for the minimum surface roughness and maximum production rate.

However, many other previous works have focused on the determination of the optimal cutting conditions for different objectives [20–27]. Zuperl and Cus [20] described a method for optimizing multi-purpose turning cutting conditions with the help of neural networks aimed at increasing productivity and reducing costs, and providing an acceptable surface roughness. Senthilkumaar et al. [21] derived a mathematical model and ANN model for tool wear and surface roughness Ra for turning heat-resistant super alloy Inconel 718 material. Optimal processing parameters were selected using the Pareto chart. Zinati and Razfar [22] derived prediction models for cutting conditions that ensure minimal surface roughness for longitudinal turning (turning long parts) of X20Cr13. Jafarian et al. [23] investigated three separate neural networks in order to minimize the surface roughness and maximize tool life in the turning. Mokhtari Homami et al. [24] reported optimal values of flank wear and surface roughness with the use of neural networks for turning Inconel718 superalloy components. Tamang and Chandrasekaran [25] used artificial neural networks for optimal cutting conditions, ensuring minimum values of surface roughness and tool wear on the rear surface for turning Al/SiCp MMC. Sangwan et al. [26] used artificial neural networks (ANN) and genetic algorithm (GA) to

obtain the optimum processing parameters leading to minimal surface roughness when turning a titanium alloy Ti-6Al-4 V. Gupta et al. [27] focused on the optimization of the process parameters of turning operations, namely surface roughness, the back surface of tool wear and power consumption. However, in the abovementioned research [20–27] the task of finding the optimum cutting conditions is one-sided, taking into account only the surface roughness without its relationship to the productivity and machining time of unit volume, which does not present the optimum handling of an expensive material such as high-strength steel.

Now, we consider the work focused on the determination of optimal parameters for turning with multi-objective optimization [28–31]. Basak et al. [28] discussed two types of Pareto optimization: minimizing the production time and minimizing the cost of processing, while the surface roughness was considered as a limiting parameter. Karpat and Özel [29] used neural networks based on multi-objective Pareto optimization modes for longitudinal turning of hardened AISI H13 steel. Two optimization criteria were investigated: the minimization of surface roughness values and maximization of performance in terms of longer tool life and material removal rate, while the second criterion was devoted to minimizing the processing-induced stress on the surface and minimum surface roughness. Yue et al. [30], based on multi-objective Pareto optimization for hard turning of die steel Cr12MoV, established a relationship between surface roughness, thickness of the plastic deformation zone, and cutting modes. Abbas et al. [31] studied the turning parameters for a heat-treated steel alloy (J-Steel) through multi-criteria optimization with the help of Pareto optimization. The work reported the cutting parameters that provided the minimum surface roughness and machining time needed to remove a unit volume. It can be concluded that the most effective approach to solving multi-objective optimization is the Pareto method. However, of the references mentioned here [28–31], none have considered multi-criteria optimization for the turning of high-strength steel, which is a material that is widely used in critical applications where there are stringent requirements on surface quality. Besides, due to the high cost of this material, it should be guaranteed to ensure the desired machined surface roughness value along with the minimum amount of processing time to promote productivity.

Thus, the aim of this study is to determine the turning conditions for high-strength steel while providing the minimum machining time of unit volume T_m and the required value of surface roughness Ra by using an artificial neural network-based model for prediction of these parameters.

2 Materials and methods

The chemical composition and mechanical properties of high-strength steel used in the current study are shown in Tables 1 and 2, respectively. This type of steel belongs to British Military of Defense (defense standard number:10–13/3 (2012)). The heat treatment for the material involved austenitizing at 900 °C for 5 h, air cooling, heating at 880 °C for 5 h, quenching in oil, and finally tempering at 590–600 °C for 8 h, followed by air cooling. The hardness measured was about HV 410 ± 10.

The test specimen had an initial diameter d of 50 mm and a length of 120 mm. Thirty millimeters was used for chuck clamping and 10 mm for clearance grooving and 60 mm will be used for applying the test experiment. A standard conical center was created for supporting the center of the tail stock.

The EMCO Concept Turn lathe 45 CNC equipped with Sinumeric 840-D was used to conduct the experimental work (Fig. 1).

The uncoated tungsten carbide insert was clamped with the tool holder to carry out this experiment. The specifications for the insert and tool holder are SVJCL2020K16 and VCMT160404 (back angle $\alpha = 7^\circ$, cutting edge angle $k_r = 75^\circ$, nose radius $r_o = 0.4$ mm). The surface roughness was measured and reported for a length of 50 mm, and evaluated using the surface roughness tester Tessa (Fig. 2). All the cutting parameters were controlled via the CNC part program [19].

To ensure a richly dense exploration of the adjustable space of the cutting parameters, a five-level full factorial design of experiments (total of 125 test conditions for three study parameters) was adopted. Listing of the factor levels for the study parameters is provided in Table 3.

For efficient experimentation, the 125 samples were divided into five primary groups (with the same cutting speed for each primary group), each of which was divided into five sub-groups (each having the same depth of cut). A full listing of all the resulting measured surface roughness values is provided in the Section 4.

3 The strategy for determining the optimum conditions

To achieve our objective, it is necessary to build an artificial neural network-based model of turning based on experimental data [32–34] and solve the optimization

Table 1 Chemical composition of the high-strength steel material

Element	C	Si	Mn	Ni	Cr	Mo	V	S	P
%	0.32	0.23	0.64	3.02	0.96	0.48	0.12	0.002	0.004

Table 2 Mechanical properties of the high-strength steel work piece

Elastic modulus, E , GPa	0.2% yield strength, MPa	Ultimate tensile strength, MPa	Area reduction, %	Elongation, %
206	1114	1195	59	9.3

problem in a multi-criteria environment using the Edgeworth and Pareto method [28–31, 35–38].

The strategy for determining the optimum conditions is realized in five steps:

- *Step one*

Set the optimization criteria, define the limitations and boundary conditions. Define the vector space of the problem being solved.

- *Step two*

Using the data mining approach [39–42], carry out three variables functions approximation based on experimental data with the help of the neural network.

- *Step three*

Determine the Pareto frontier: the set of Pareto optimal decisions and the set of Pareto optimal estimates.

- *Step four*

Using the expert assessment method, narrow the scope of Pareto optimality to Pareto non-dominated decisions.

- *Step five*



Fig. 1 Test rig for machining samples

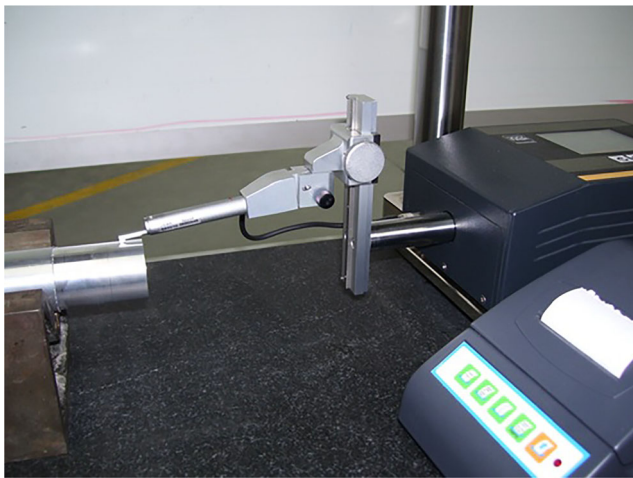


Fig. 2 Test rig measuring surface roughness

Apply the decision-maker’s direct questioning to establishing a set of selected decisions that may only contain a single optimum decision with a single estimates vector.

The strategy for decision-making in a multi-criterion selection problem is presented in Fig. 3 and the correlation of vector estimate sets is presented in Fig. 4. The nomenclature used in the charts and later on is the same as in [43]: DM—decision maker; m —the number of criteria; $I = \{1, 2, \dots, m\}$ —a set of criteria numbers; X – a set of possible decisions; $f = (f_1, f_2, \dots, f_m)$ – vector-valued criterion; $Y = f(X)$ —a set of possible vectors (estimates); R^m —Euclidean space of m -dimensional vectors with real components; \succ_X —preference relation of DM specified in the set X ; \succ_Y —preference relation of DM, induced on the set with \succ_X ratio and specified in the set Y ; \succ —relation \succ_Y continued in the entire space R^m ; Sel X —a set of selected decisions; Sel Y —a set of selected vectors (estimates); Ndom X —a set of non-dominated decisions; Ndom Y —a set of non-dominated vectors (estimates); $P_f(X)$ —a set of Pareto optimal decisions; $P(Y)$ —a set of Pareto optimal vectors (Pareto optimal estimates).

Table 3 Factor levels of the full factorial experimentation

Factor/factor level	Cutting speed, V (m/min)	Depth of cut, t (mm)	Feed rate, f_z (mm/rev)
1	75	0.1	0.025
2	100	0.2	0.050
3	125	0.3	0.100
4	150	0.4	0.150
5	175	0.5	0.200

4 Results and discussion

Besides surface quality, the problem of minimizing resource consumption becomes very important in finish turning of expensive high-strength steel. It is crucial to provide the minimum machining time of unit volume T_m and minimum surface roughness Ra at the same time. That is why these two criteria are the most important for finding the optimum machining parameters.

The results of experiments are presented in Tables 4, 5, 6, 7, and 8. Surface roughness (Ra , μm) was established experimentally, and the second criterion (machining time of unit volume, T_m , min/cm^3) was calculated with the following formula:

$$T_m = \frac{1000}{V \cdot t \cdot f_z} \tag{1}$$

Thus, on the researcher level, the first three steps were implemented.

The optimization problem was solved using the five-step strategy presented earlier.

4.1 Formulation of the optimization problem—step 1

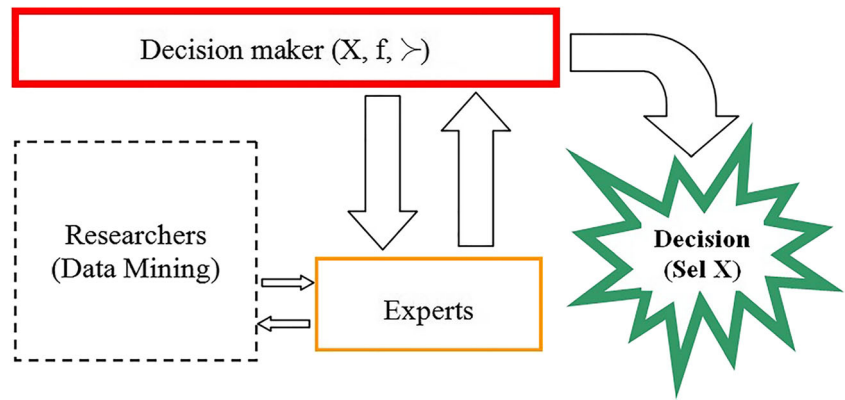
Based on the research objective, the following criteria in turning of the cylindrical workpiece were established: f_1 —surface roughness, Ra , μm ; f_2 —machining time of unit volume in one cutting tool pass, T_m , min/cm^3 , that is, $m = 2$. Relatively, a set of possible Y estimates in the two-dimensional space R^2 forms the vectors $f = (f_1, f_2)$. The search is performed for a set of estimates having the minimum sum of vector lengths throughout the entire range of the criteria values changes. For this purpose, it makes sense to present them in a dimensionless form with the index “1” assigned to the maximum actual numbers.

Variable parameters and limitations of the optimization problem were set in accordance with the table of experimental data (see Table 3): $x_1 = [75-175]$ —cutting speed, V , m/min; $x_2 = [0.1-0.5]$ —depth of cut, t , mm; $x_3 = [0.025-0.20]$ —feed per revolution, f_z , mm per rev.

For the optimization procedure, dimensionless surface roughness f_1 (Ra^*) and machining time of unit volume f_2 (T_m^*) (Tables 4, 5, 6, 7, and 8) were calculated using the following formulae:

$$Ra^* = \frac{Ra_i}{Ra_{\max}}; \tag{2}$$

Fig. 3 The decision tree in the multi-criterion selection problem



$$T_m^* = \frac{T_{mi}}{T_{mmax}}, \tag{3}$$

where Ra_t —surface roughness for current V, t and f_z parameter combinations; Ra_{max} —maximum surface roughness value of all the V, t and f_z combinations; $T_{mi}T_{mi}$ —machining time of unit volume for current V, t and f_z parameter combinations; T_{mmax} —maximum machining time of unit volume value of all the V, t and f_z combinations. The length of estimates vector f was established with the Pythagorean theorem using dimensionless criteria f_1 and f_2 .

The problem boundary condition was that all variables can take any non-negative values.

Since the criterion of the machining time of unit volume T_m^* was calculated, in the second stage of our strategy, the function of surface roughness $Ra^* = f(x_1, x_2, x_3)$ needed approximation.

Figure 5 shows a three-dimensional surface built on the basis of the experimental points (see Table 8) that reflects the non-linear changes in surface roughness given the changing cutting speed V and feed rate f_r with fixed depth of cut $t = 0.5$ mm.

At the stage of performing a regression analysis of the experimental data, a non-linear association has been established represented by a four-dimensional paraboloid with determination coefficient $R^2 = 0.957$ (with $\pm 4.21\%$ accuracy):

$$Ra = -0.15 + 0.09V + 0.12t + 0.17f_r + 0.25V^2 + 0.29t^2 + 0.17f_r^2. \tag{4}$$

Using this non-linear function helped us establish that increasing the coded value of V by 0.1 points leads to an 0.036-point increase of surface roughness ($0.137 \mu\text{m}$); increasing the coded value of t leads to a 0.047-point increase in surface roughness ($0.177 \mu\text{m}$), and increasing the coded value of f_r by 0.1 points leads to a 0.037-point ($0.140 \mu\text{m}$) increase in surface roughness. So, as compared with the influence of V on surface roughness, depth of cut t has a 25.9% greater effect on it, and feed rate f_r has a 1.9% greater effect.

Considering the complicated and non-linear nature of the emergence of this parameter, we had to employ the capacities of the SKIF Aurora-SUSU supercomputer cluster (South Ural State University, Chelyabinsk, Russia) [44].

4.2 Creation of a surface roughness prediction model using an artificial neural network—step 2

Among the most popular packages—Maple, Mathematica, Mathcad, and Matlab—only Matlab today is intended for fundamental, high quality and versatile numeric calculations. The toolbox for creating, training and modeling of neural networks (the Neural Network Toolbox) in Matlab makes it much simpler to

Fig. 4 The relations of sets of vector estimates: the largest set is the set of possible estimates Y , and the smallest—a set of selected vectors $Sel Y$

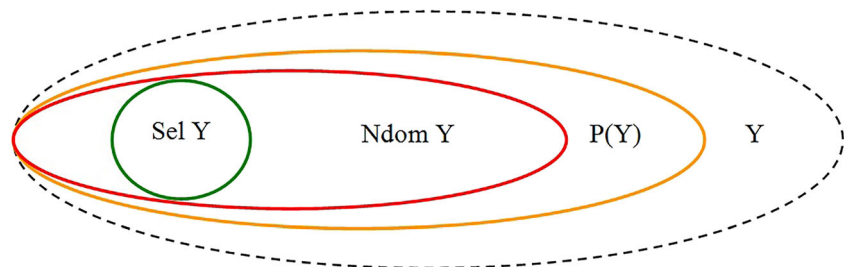


Table 4 Optimization criteria values for variable workpiece turning parameters at the depth of cut $t = 0.1$ mm

Variable parameters				Optimization criteria				
x_1 Cutting speed, V (m/min)	x_2 Depth of cut, t (mm)	x_3 Feed rate, f_z (mm/rev)	Results of experiment			Dimensionless criteria		
			Surface roughness, Ra (μm)	Machining time of unit volume, T_m (min/cm ³)	Machining time of unit volume f_2 (T_m^*), unit	Surface roughness f_1 (Ra^*), unit	Estimated vector length, f , unit	
75	0.1	0.025	0.602	5.333	1	0.16	1.013	
75	0.1	0.05	0.202	2.667	0.5	0.054	0.503	
75	0.1	0.1	0.827	1.333	0.25	0.219	0.332	
75	0.1	0.15	1.616	0.889	0.167	0.428	0.459	
75	0.1	0.2	2.924	0.667	0.125	0.775	0.785	
100	0.1	0.025	0.348	4	0.75	0.092	0.756	
100	0.1	0.05	0.287	2	0.375	0.076	0.383	
100	0.1	0.1	0.957	1	0.188	0.254	0.316	
100	0.1	0.15	1.746	0.667	0.125	0.463	0.48	
100	0.1	0.2	2.393	0.5	0.094	0.634	0.641	
125	0.1	0.025	0.458	3.2	0.6	0.121	0.612	
125	0.1	0.05	0.375	1.6	0.3	0.099	0.316	
125	0.1	0.1	0.703	0.8	0.15	0.186	0.239	
125	0.1	0.15	1.795	0.533	0.1	0.476	0.486	
125	0.1	0.2	3.212	0.4	0.075	0.851	0.854	
150	0.1	0.025	0.47	2.667	0.5	0.125	0.515	
150	0.1	0.05	0.563	1.333	0.25	0.149	0.291	
150	0.1	0.1	1.068	0.667	0.125	0.283	0.309	
150	0.1	0.15	1.675	0.444	0.083	0.444	0.452	
150	0.1	0.2	2.502	0.333	0.062	0.663	0.666	
175	0.1	0.025	0.662	2.286	0.429	0.175	0.463	
175	0.1	0.05	0.629	1.143	0.214	0.167	0.271	
175	0.1	0.1	0.821	0.571	0.107	0.218	0.243	
175	0.1	0.15	1.581	0.381	0.071	0.419	0.425	
175	0.1	0.2	2.435	0.286	0.054	0.645	0.647	

Table 5 Optimization criteria values for variable workpiece turning parameters at the depth of cut $t = 0.2$ mm

Variable parameters			Optimization criteria				
x_1 Cutting speed, V (m/min)	x_2 Depth of cut, t (mm)	x_3 Feed rate, f_z (mm/rev)	Results of experiment			Dimensionless criteria	
			Surface roughness, Ra (μm)	Machining time of unit volume, T_m (min/cm ³)	Dimensionless surface roughness f_1 (Ra^*), unit	Dimensionless machining time of unit volume f_2 (T_m^*), unit	Estimated vector length, f , unit
75	0.2	0.025	0.141	2.667	0.037	0.5	0.501
75	0.2	0.05	0.266	1.333	0.07	0.25	0.26
75	0.2	0.1	0.807	0.667	0.214	0.125	0.248
75	0.2	0.15	1.599	0.444	0.424	0.083	0.432
75	0.2	0.2	3.774	0.333	1	0.062	1.002
100	0.2	0.025	0.228	2	0.06	0.375	0.38
100	0.2	0.05	0.314	1	0.083	0.188	0.206
100	0.2	0.1	0.771	0.5	0.204	0.094	0.225
100	0.2	0.15	1.622	0.333	0.43	0.062	0.434
100	0.2	0.2	2.789	0.25	0.739	0.047	0.74
125	0.2	0.025	0.515	1.6	0.136	0.3	0.329
125	0.2	0.05	0.842	0.8	0.223	0.15	0.269
125	0.2	0.1	1.981	0.4	0.525	0.075	0.53
125	0.2	0.15	2.025	0.267	0.537	0.05	0.539
125	0.2	0.2	2.778	0.2	0.736	0.038	0.737
150	0.2	0.025	0.671	1.333	0.178	0.25	0.307
150	0.2	0.05	0.378	0.667	0.1	0.125	0.16
150	0.2	0.1	0.965	0.333	0.256	0.062	0.263
150	0.2	0.15	1.636	0.222	0.433	0.042	0.435
150	0.2	0.2	2.225	0.167	0.59	0.031	0.591
175	0.2	0.025	0.832	1.143	0.22	0.214	0.307
175	0.2	0.05	0.365	0.571	0.097	0.107	0.144
175	0.2	0.1	0.857	0.286	0.227	0.054	0.233
175	0.2	0.15	1.67	0.19	0.443	0.036	0.444
175	0.2	0.2	2.649	0.143	0.702	0.027	0.703

Table 6 Optimization criteria values for variable workpiece turning parameters at the depth of cut $t = 0.3$ mm

Variable parameters				Optimization criteria				
x_1 Cutting speed, V (m/min)	x_2 Depth of cut, t (mm)	x_3 Feed rate, f_z (mm/rev)	Results of experiment			Dimensionless criteria		
			Surface roughness, Ra (μm)	Machining time of unit volume, T_m (min/cm ³)	Machining time of unit volume f_2 (T_m^*), unit	Surface roughness f_1 (Ra^*), unit	Estimated vector length, f , unit	
75	0.3	0.025	0.277	1.778	0.333	0.073	0.341	
75	0.3	0.05	0.297	0.889	0.167	0.079	0.185	
75	0.3	0.1	0.996	0.444	0.083	0.264	0.277	
75	0.3	0.15	1.703	0.296	0.056	0.451	0.454	
75	0.3	0.2	2.907	0.222	0.042	0.77	0.771	
100	0.3	0.025	0.402	1.333	0.25	0.107	0.272	
100	0.3	0.05	0.437	0.667	0.125	0.116	0.171	
100	0.3	0.1	0.775	0.333	0.062	0.205	0.214	
100	0.3	0.15	1.386	0.222	0.042	0.367	0.369	
100	0.3	0.2	3.223	0.167	0.031	0.854	0.855	
125	0.3	0.025	1.063	1.067	0.2	0.282	0.346	
125	0.3	0.05	0.588	0.533	0.1	0.156	0.185	
125	0.3	0.1	1.575	0.267	0.05	0.417	0.42	
125	0.3	0.15	2.054	0.178	0.033	0.544	0.545	
125	0.3	0.2	2.65	0.133	0.025	0.702	0.702	
150	0.3	0.025	0.547	0.889	0.167	0.145	0.221	
150	0.3	0.05	0.345	0.444	0.083	0.091	0.123	
150	0.3	0.1	0.855	0.222	0.042	0.227	0.231	
150	0.3	0.15	1.45	0.148	0.028	0.384	0.385	
150	0.3	0.2	2.458	0.111	0.021	0.651	0.651	
175	0.3	0.025	0.665	0.762	0.143	0.176	0.227	
175	0.3	0.05	0.374	0.381	0.071	0.099	0.122	
175	0.3	0.1	0.808	0.19	0.036	0.214	0.217	
175	0.3	0.15	1.753	0.127	0.024	0.464	0.465	
175	0.3	0.2	2.059	0.095	0.018	0.546	0.546	

Table 7 Optimization criteria values for variable workpiece turning parameters at the depth of cut $t = 0.4$ mm

Variable parameters			Optimization criteria					
x_1 Cutting speed, V (m/min)	x_2 Depth of cut, t (mm)	x_3 Feed rate, f_z (mm/rev)	Results of experiment			Dimensionless criteria		
			Surface roughness, R_a (μm)	Machining time of unit volume, T_m (min/cm ³)	Machining time of unit volume f_2 (T_m^*), unit	Surface roughness f_1 (R_a^*), unit	Estimates vector length, f , unit	
75	0.4	0.025	0.232	1.333	0.061	0.25	0.257	
75	0.4	0.05	0.252	0.667	0.067	0.125	0.142	
75	0.4	0.1	0.88	0.333	0.233	0.062	0.241	
75	0.4	0.15	1.996	0.222	0.529	0.042	0.531	
75	0.4	0.2	3.068	0.167	0.813	0.031	0.814	
100	0.4	0.025	0.237	1	0.063	0.188	0.198	
100	0.4	0.05	0.257	0.5	0.068	0.094	0.116	
100	0.4	0.1	0.64	0.25	0.17	0.047	0.176	
100	0.4	0.15	1.398	0.167	0.37	0.031	0.371	
100	0.4	0.2	2.446	0.125	0.648	0.023	0.648	
125	0.4	0.025	0.393	0.8	0.104	0.15	0.183	
125	0.4	0.05	0.636	0.4	0.169	0.075	0.185	
125	0.4	0.1	1.365	0.2	0.362	0.038	0.364	
125	0.4	0.15	1.713	0.133	0.454	0.025	0.455	
125	0.4	0.2	2.375	0.1	0.629	0.019	0.629	
150	0.4	0.025	0.495	0.667	0.131	0.125	0.181	
150	0.4	0.05	0.269	0.333	0.071	0.062	0.095	
150	0.4	0.1	0.866	0.167	0.229	0.031	0.231	
150	0.4	0.15	1.715	0.111	0.454	0.021	0.454	
150	0.4	0.2	2.317	0.083	0.614	0.016	0.614	
175	0.4	0.025	0.358	0.571	0.095	0.107	0.143	
175	0.4	0.05	0.423	0.286	0.112	0.054	0.124	
175	0.4	0.1	0.869	0.143	0.23	0.027	0.232	
175	0.4	0.15	1.786	0.095	0.473	0.018	0.473	
175	0.4	0.2	2.635	0.071	0.698	0.013	0.698	

Table 8 Optimization criteria values for variable workpiece turning parameters at the depth of cut $t = 0.5$ mm

Variable parameters			Optimization criteria				
x_1 Cutting speed, V (m/min)	x_2 Depth of cut, t (mm)	x_3 Feed rate, f_z (mm/rev)	Results of experiment		Dimensionless criteria		
			Surface roughness, R_a (μm)	Machining time of unit volume, T_m (min/cm ³)	Surface roughness f_1 (Ra^*), unit	Machining time of unit volume f_2 (T_m^*), unit	Estimated vector length, f , unit
75	0.5	0.025	0.32	1.067	0.085	0.2	0.217
75	0.5	0.05	0.298	0.533	0.079	0.1	0.127
75	0.5	0.1	0.984	0.267	0.261	0.05	0.266
75	0.5	0.15	1.71	0.178	0.453	0.033	0.454
75	0.5	0.2	2.996	0.133	0.794	0.025	0.794
100	0.5	0.025	0.147	0.8	0.039	0.15	0.155
100	0.5	0.05	0.247	0.4	0.065	0.075	0.099
100	0.5	0.1	0.753	0.2	0.2	0.038	0.204
100	0.5	0.15	1.5	0.133	0.397	0.025	0.398
100	0.5	0.2	2.31	0.1	0.612	0.019	0.612
125	0.5	0.025	0.367	0.64	0.097	0.12	0.154
125	0.5	0.05	0.633	0.32	0.168	0.06	0.178
125	0.5	0.1	1.135	0.16	0.301	0.03	0.302
125	0.5	0.15	1.721	0.107	0.456	0.02	0.456
125	0.5	0.2	2.436	0.08	0.645	0.015	0.645
150	0.5	0.025	0.332	0.533	0.088	0.1	0.133
150	0.5	0.05	0.307	0.267	0.081	0.05	0.094
150	0.5	0.1	0.91	0.133	0.241	0.025	0.242
150	0.5	0.15	1.644	0.089	0.436	0.017	0.436
150	0.5	0.2	2.337	0.067	0.619	0.013	0.619
175	0.5	0.025	0.441	0.457	0.117	0.086	0.145
175	0.5	0.05	0.477	0.229	0.126	0.043	0.133
175	0.5	0.1	0.745	0.114	0.197	0.021	0.198
175	0.5	0.15	1.92	0.076	0.509	0.014	0.509
175	0.5	0.2	2.487	0.057	0.659	0.011	0.659

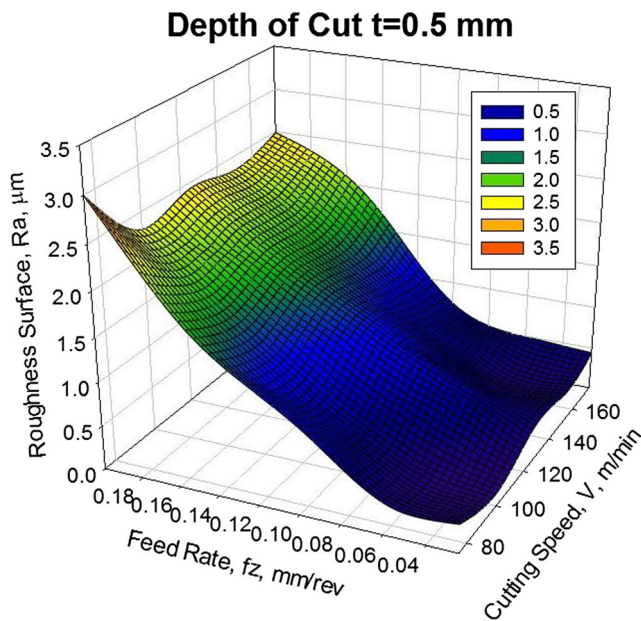
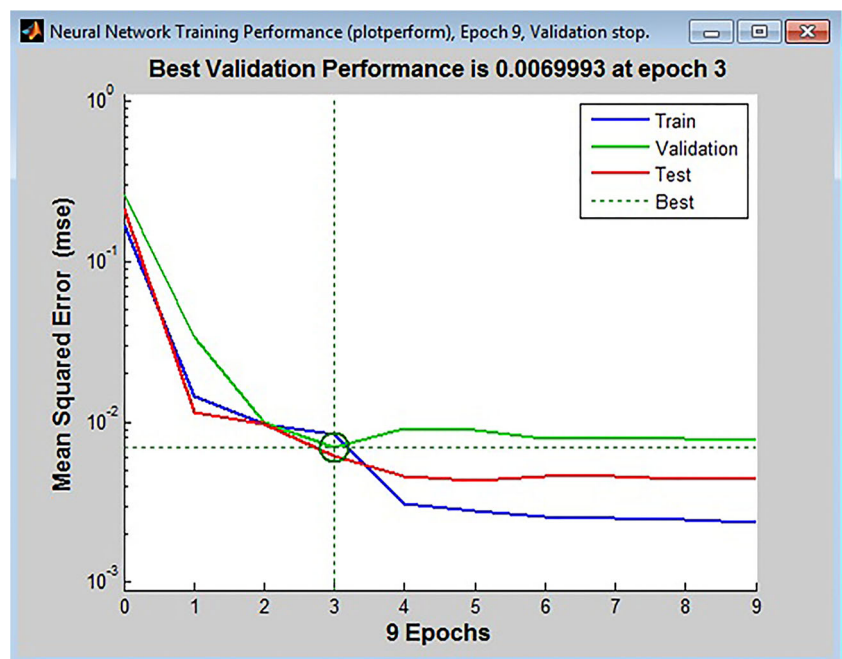


Fig. 5 Three-dimensional surface built on the basis of the experimental points reflecting the non-linear changes in surface roughness given the changing cutting speed V and feed rate f_r with fixed depth of cut $t = 0.5$ mm

create neural networks. An undeniable advantage of Matlab is its language, which allows users to create their own algorithms and applications. The multi-purpose nature of the language provides opportunities for accomplishing a number of tasks such as collecting, analyzing and structuring data, developing algorithms, modeling systems, object-oriented programming, development of a graphical user interface, debugging and converting Matlab applications to C or C++ codes. That is why a parallel version of

Fig. 6 The lowest mean squared error for the validation set in MLP 3-9-1 configuration (calculated in Matlab)



Matlab R2010b was chosen as the programming environment for this study.

The controlled feedforward neural network was trained based on a multilayer perceptron (MLP) using the Levenberg–Marquardt algorithm. The network structure included a hidden layer of sigmoid neurons and a linear layer of output neurons, because this is the best structure for multi-dimensional mapping problems.

The preliminary processing of data, which consisted in normalization of the values similar to the normalization of dimensionless criteria (see formulae 2 and 3), provided for compliance of the input values with the $[0,1]$ range and was carried out with the aim of improving the efficiency of the network training process.

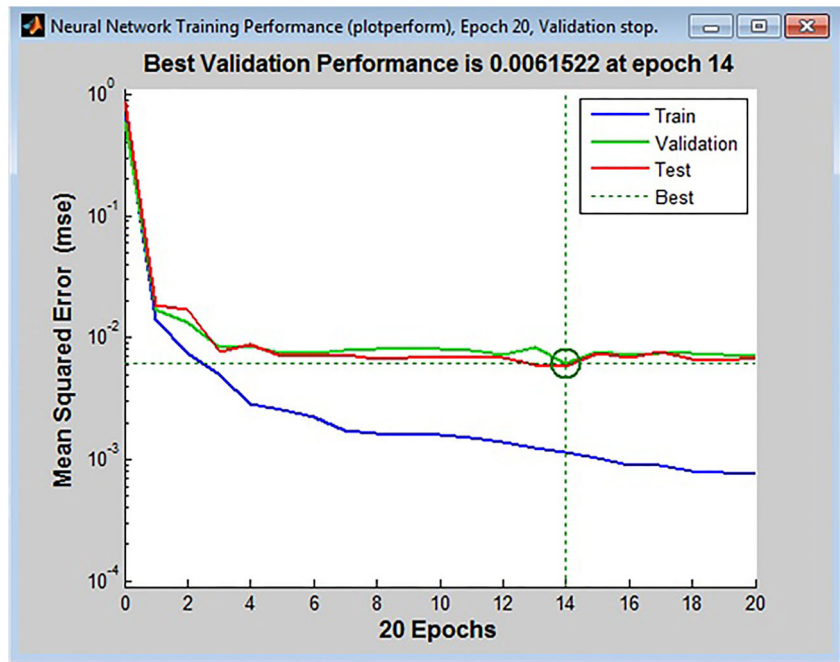
The overfitting problem was solved by improving the generalization performance of the network. To do that, two data sets were used: the training set for updating weights and offsets; and the validation set for stopping the training if an undesirable event occurs.

The final configuration (the number of neurons in the hidden layer) of the network was established based on the lowest mean squared error in the validation set.

To begin with, the multilayer perceptrons were trained with nine, ten, and 11 neurons in the hidden layer, with 15% of the tabular data allocated to the validation set. The lowest error values for MLP 3-9-1, MLP 3-10-1, and MLP 3-11-1 are presented in Figs. 6, 7, and 8 respectively.

Analysis of the graphical functions presented in Figs. 6, 7 and 8 showed that the lowest error of 0.61% in the validation set was provided by the MLP 3-10-1 network structure. The coefficient of determination of the obtained model was 0.978,

Fig. 7 The lowest mean squared error for the validation set in MLP 3–10–1 configuration (calculated in Matlab)



which reflects its high accuracy in predicting surface roughness ($\pm 2.14\%$). The same structure appeared to give the best generalization performance in the cases of allocating 10 or 20% in the validation set of tabular data (Fig. 9). In the first training variant, the error was 0.86% (see Fig. 9b) and in the second variant, it was 1.00% (see Fig. 9c).

4.3 Establishing a Pareto frontier—step 3

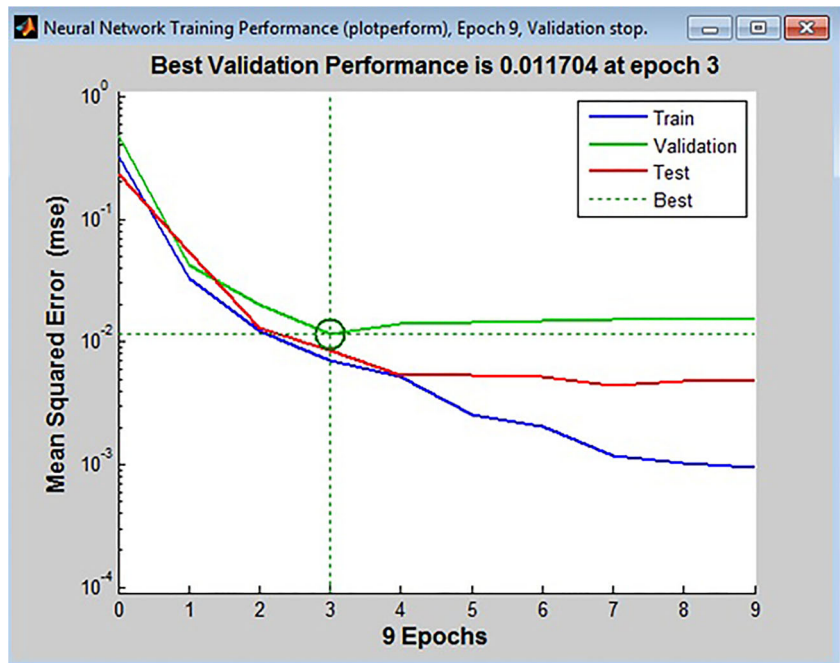
The third step of the strategy involved calculating the values of Ra^* for the experimental values x_1, x_2, x_3 (see Tables 4, 5,

6, 7, and 8) with the help of the network and plotting charts of dimensionless criteria relations taking into account the T_m^* values (Fig. 10).

Intercept AB for cutting depth $t = 0.5$ mm with varying $V = 150 \dots 175$ m/min and $f_z = 0.025 \dots 0.085$ mm/rev was plotted between the tangency points of the line and the lowest curves (Fig. 11). The coordinates of the intercept ends were A (0,113; 0,034) and B (0,204; 0,022).

Considering the downward trend of the target function f , there are six reference points of the Pareto frontier (Fig. 12). In the new numbering, point A is given number 4 and point B—number 5.

Fig. 8 The lowest mean squared error for the validation set in MLP 3–11–1 configuration (calculated in Matlab)



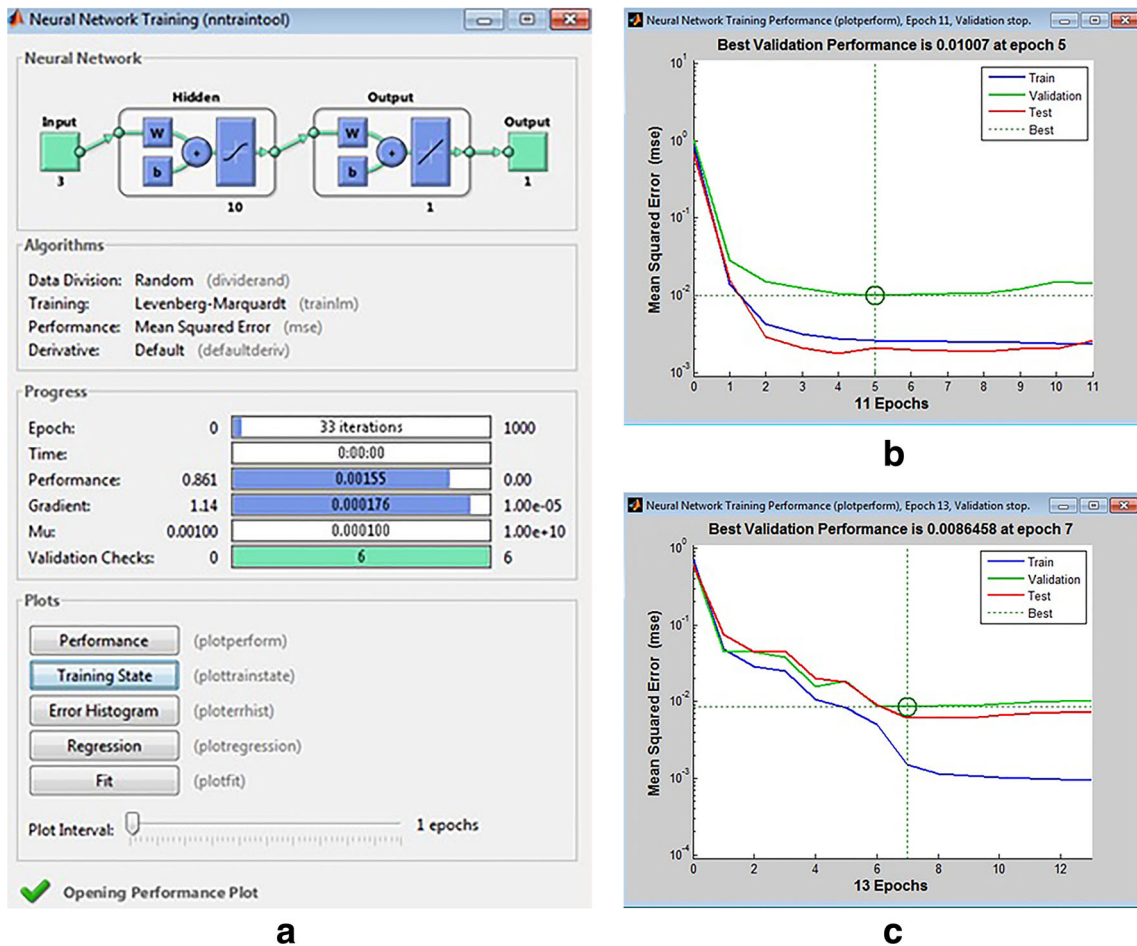


Fig. 9 The lowest mean squared error in generalizing experimental data in MLP 3–10–1(a) with various validation sets: b–10%, c–20% (calculated in Matlab)

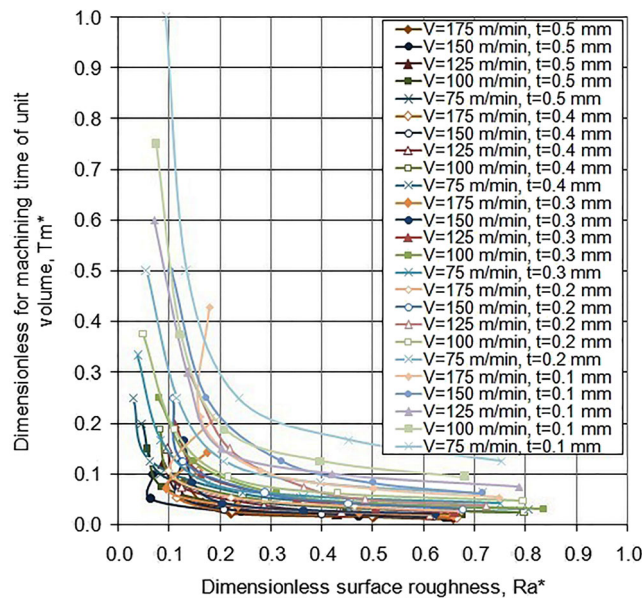


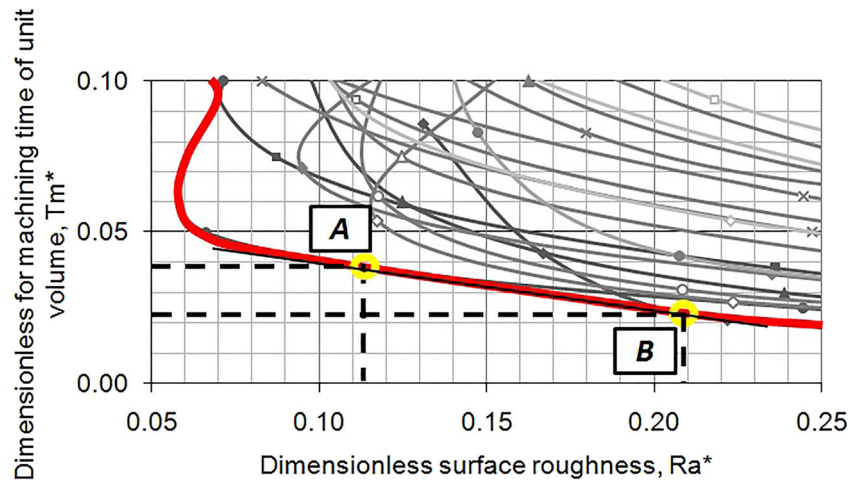
Fig. 10 Graphs showing the relation of dimensionless machining time of unit volume T_m^* with dimensionless surface roughness Ra^* for fixed depth of cut t and cutting speed V with varying feeds per revolution (with increasing feed, Ra^* increases and T_m^* decreases)

Analysis of the Pareto curve allowed us to establish five sections. Section I between points 1 and 2 corresponds to $t = 0.4$ mm and $V = 70$ m/min. Section II between points 2 and 3 corresponds to $t = 0.5$ mm and $V = 100$ m/min. Section III between points 3 and 4 corresponds to $t = 0.5$ mm and $V = 150$ m/min. Section IV between points 4 and 5 has been presented before (see Fig. 11). Section V between points 5 and 6 corresponds to $t = 0.5$ mm and $V = 175$ m/min. Points 1 and 6 are the end points of relations $t = 0.4$ mm at $V = 75$ m/min and $t = 0.5$ mm at $V = 175$ m/min, respectively.

4.4 Establishment of Pareto non-dominated decisions—step 4

In accordance with the strategy, step four involved narrowing the set of Pareto optimal decisions to a set of Pareto non-dominated decisions. For this purpose, the method of expert assessments was used to establish greater importance of the dimensionless criterion of the machining time of unit volume T_m^* over the

Fig. 11 Coordinates of points A and B of the tangent to the curve showing the relation between dimensionless criteria for depth of cut $t = 0.5$ mm with varying cutting speed V and feed per revolution f_z in the ranges of 150 through 175 m/min and 0.025 to 0.085 mm/rev, respectively.



dimensionless criterion of surface roughness Ra^* . As a result, Pareto non-dominated estimates are presented by all vectors located below the blue one, taking into account the equivalence of f_1 and f_2 and plotted at 45° angle to the reference axes (Fig. 13). The end point of this vector with the coordinates (0.054, 0.054) (point 7 in the Pareto frontier) became the global minimum in the case of unconditional optimization with equivalent criteria f_1 and f_2 . In the actual coordinates, the global minimum in the case of equivalent criteria of the machining time of unit volume T_m^* and roughness Ra^* corresponds to the following values: $T_m = 0.287$ min/cm³, $Ra = 0.203$ μ m, $V = 150$ m/min, $t = 0.5$ mm and $f_z = 0.043$ mm/rev.

4.5 Establishment of the optimum cutting conditions—step 5

In the fifth and final step of the implemented optimization strategy, direct questioning of the decision-maker (chief designer) set the maximum allowable roughness value. It is $Ra = 0.8$ μ m or the eighth point on the Pareto frontier curve, with the coordinates (0.212, 0.021), as shown in Fig. 14. In this case (the green estimates vector in Fig. 12), the valid relation of the importance of the optimization criteria was estimated at $T_m^*/Ra^* = 1/9$, i.e. T_m^* has a ninefold differential

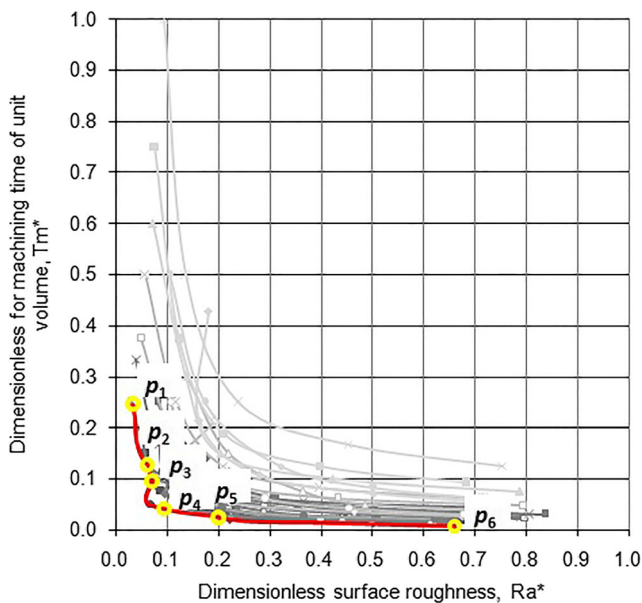


Fig. 12 Six reference points of the Pareto frontier

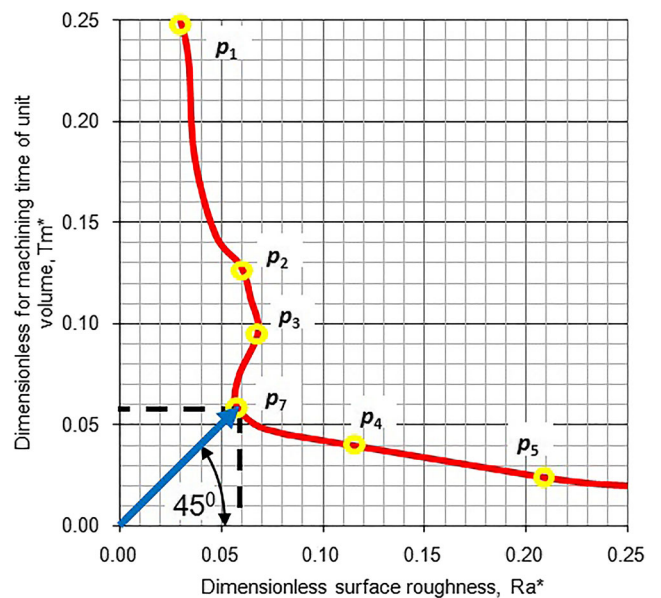


Fig. 13 The global minimum vector of the Pareto optimality function in the case of equivalent machining time of unit volume T_m^* and surface roughness Ra^* (the actual parameters of the global minimum are reflected by the blue vector: $T_m = 0.287$ min/cm³, $Ra = 0.203$ μ m, $V = 150$ m/min, $t = 0.5$ mm and $f_z = 0.043$ mm/rev)

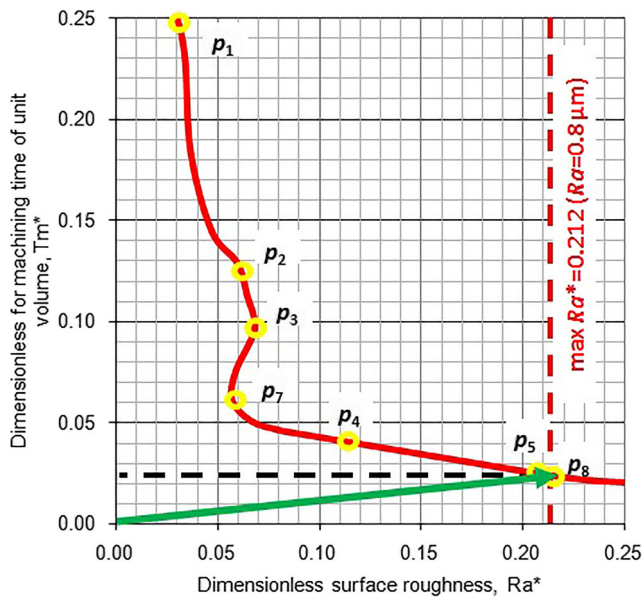


Fig. 14 Vector of the global minimum of Pareto optimal function in the case of machining time of unit volume T_m^* being nine times as important as surface roughness Ra^* (the actual parameters of the global minimum are presented by the green vector: $T_m = 0.111 \text{ min/cm}^3$, $R_a = 0.8 \text{ }\mu\text{m}$, $V = 150 \text{ m/min}$, $t = 0.5 \text{ mm}$ and $f_z = 0.112 \text{ mm/rev}$)

over R_7 and 8 and a valid preference is $y_8 > y_7$ and induced $x_8 > x_7$.

As a result, the set of selected estimates Sel Y became limited to the green vector with the end actual coordinates (0.212, 0.021) and the set of selected decisions Sel X to the three-dimensional vector of the optimum cutting conditions ($f_z = 0.112$, $t = 0.5$, $V = 150$).

To sum up, it should be noted that accurate values of the points on the Pareto curve and the coordinates of the presented vectors have been obtained automatically in Matlab using a neural network model as a custom function. In particular, estimates vector f has been chosen as the optimization criteria, the limitation is the ratio of T_m^* : $Ra^* = 9: 1$, and the boundary conditions are positive values of cutting speed V , cutting depth t and feed rate f_z . The non-linear constrained optimization problem was solved using the Newton method with quadratic convergence. The program implementation of the presented strategy in Matlab allows the quick calculation of the local optimum parameters of cutting conditions with various computer-aided manufacturing complexes for the whole range of cutting speeds and depths.

5 Conclusions

- (1) A five-step methodology for optimizing multifactorial systems has been presented to find the best solution for the set of experimental data.
- (2) For the first time for turning of high-strength steel, the Edgeworth-Pareto methodology of searching for the

optimum in a multi-criterion environment was used and made it possible to find the best conditions in the n -dimensional decision space clearly and promptly using a neural network-based model.

- (3) An artificial neural network was created in the Matlab programming environment based on the MLP 3-10-1 multilayer perceptron, which predicts the surface roughness of a cylindrical workpiece with a diameter of $\varnothing 50$ and length of 120 mm manufactured from high-strength steel after finish turning in the following ranges of parameters: cutting speed from 75 through 175 m/min, depth of cut from 0.1 to 0.5 mm and feed per revolution of 0.025 to 0.20 mm with the accuracy of $\pm 2.14\%$.
- (4) The global optimum for turning high-strength steel with the required surface roughness of the end workpiece was established: the required value of surface roughness $R_a = 0.8 \text{ }\mu\text{m}$ and the minimum machining time of unit volume $T_m = 0.111 \text{ min/cm}^3$ correspond to the optimum conditions of finish turning: cutting speed $V = 174 \text{ m/min}$, cutting depth $t = 0.55 \text{ mm}$ and feed $f_z = 0.112 \text{ mm/rev}$.
- (5) Using Matlab, conditions were created for automating the design of the optimum turning conditions in the turning of high-strength steel and for integrating artificial intelligence into the CNC machine management system.

Acknowledgments This project was supported by King Saud University, Deanship of Scientific Research, College of Engineering Research Center.

The work was supported by Act 211 Government of the Russian Federation, contract no. 02.A03.21.0011.

The research was carried out within the South Ural State University Project 5-100 from 2016 to 2020 aimed to increase the competitiveness of leading Russian universities among the world research and educational centers.

Open Access This article is distributed under the terms of the Creative Commons Attribution 4.0 International License (<http://creativecommons.org/licenses/by/4.0/>), which permits unrestricted use, distribution, and reproduction in any medium, provided you give appropriate credit to the original author(s) and the source, provide a link to the Creative Commons license, and indicate if changes were made.

References

1. Risbood KA, Dixit US, Sahasrabudhe AD (2003) Prediction of surface roughness and dimensional deviation by measuring cutting forces and vibrations in turning process. *J Mater Process Technol* 132(1–3):203–214. doi:10.1016/S0924-0136(02)00920-2
2. Bajić D, Lela B, Cukor G (2008) Examination and modelling of the influence of cutting parameters on the cutting force and the surface roughness in longitudinal turning. *Strojnicki Vestn / J Mech Eng* 54(5):322–333
3. Muthukrishnan N, Davim JP (2009) Optimization of machining parameters of Al/SiC-MMC with ANOVA and ANN analysis. *J Mater Process Technol* 209(1):225–232. doi:10.1016/j.jmatprotec.2008.01.041

4. Ali SM, Dhar NR (2010) Tool wear and surface roughness prediction using an artificial neural network (ANN) in turning steel under minimum quantity lubrication (MQL). *World Acad Sci Eng Technol* 62: 830–839
5. Pontes FJ, Ferreira JR, Silva MB, Paiva AP, Balestrassi PP (2010) Artificial neural networks for machining processes surface roughness modeling. *Int J Adv Manuf Technol* 49(9–12):879–902. doi:10.1007/s00170-009-2456-2
6. Natarajan C, Muthu S, Karuppuswamy P (2011) Prediction and analysis of surface roughness characteristics of a non-ferrous material using ANN in CNC turning. *Int J Adv Manuf Technol* 57(9–12):1043–1051. doi:10.1007/s00170-011-3343-1
7. Svalina I, Sabo K, Šimunović G (2011) Machined surface quality prediction models based on moving least squares and moving least absolute deviations methods. *Int J Adv Manuf Technol* 57(9–12): 1099–1106. doi:10.1007/s00170-011-3353-z
8. Abdullah AA, Naeem UJ, Xiong C (2012) Estimation and optimization cutting conditions of surface roughness in hard turning using Taguchi approach and artificial neural network. *Adv Mater Res* 463–464:662–668. doi:10.4028/www.scientific.net/AMR.463-464.662
9. Pontes FJ, Paiva APD, Balestrassi PP, Ferreira JR, Silva MBD (2012) Optimization of radial basis function neural network employed for prediction of surface roughness in hard turning process using Taguchi's orthogonal arrays. *Expert Syst Appl* 39(9): 7776–7787. doi:10.1016/j.eswa.2012.01.058
10. Asiltürk I (2012) Predicting surface roughness of hardened AISI 1040 based on cutting parameters using neural networks and multiple regression. *Int J Adv Manuf Technol* 63(1–4):249–257. doi:10.1007/s00170-012-3903-z
11. Upadhyay V, Jain PK, Mehta NK (2013) In-process prediction of surface roughness in turning of Ti-6Al-4V alloy using cutting parameters and vibration signals. *Measurement* 46(1):154–160. doi:10.1016/j.measurement.2012.06.002
12. Ahilan C, Kumanan S, Sivakumaran N, Edwin Raja Dhas J (2013) Modeling and prediction of machining quality in CNC turning process using intelligent hybrid decision making tools. *Appl Soft Comput* 13(3):1543–1551. doi:10.1016/j.asoc.2012.03.071
13. Azam M, Jahanzaib M, Wasim A, Hussain S (2015) Surface roughness modeling using RSM for HSLA steel by coated carbide tools. *Int J Adv Manuf Technol* 78(5-8):1031–1041. doi:10.1007/s00170-014-6707-5
14. Acayaba GMA, Escalona PMD (2015) Prediction of surface roughness in low speed turning of AISI316 austenitic stainless steel. *CIRP J Manuf Sci Technol* 11:62–67. doi:10.1016/j.cirpj.2015.08.004
15. Al Bahkali EA, Ragab AE, El Danaf EA, Abbas AT (2016) An investigation of optimum cutting conditions in turning nodular cast iron using carbide inserts with different nose radius. *Proc Inst Mech Eng B J Eng Manuf* 230(9):1584–1591 <http://dx.doi.org/10.1177/0954405416662085>
16. Mia M, Dhar NR (2016) Prediction of surface roughness in hard turning under high pressure coolant using artificial neural network. *Measurement* 92:464–474. doi:10.1016/j.measurement.2016.06.048
17. Jurkovic Z, Cukor G, Brezocnik M, Brajkovic T. (2016) A comparison of machine learning methods for cutting parameters prediction in high speed turning process. *J Intell Manuf Article in press*:1-11. doi:10.1007/s10845-016-1206-1
18. Tootooni MS, Liu C, Roberson D, Donovan R, Rao PK, Kong ZJ, Bukkapatnam STS (2016) Online non-contact surface finish measurement in machining using graph theory-based image analysis. *J Manuf Syst* 41:266–276. doi:10.1016/j.jmsy.2016.09.007
19. Abbas AT (2016) Influence of process parameters on the surface roughness during turning operation of high strength steel. *J Mater Sci Res* 5(2):1927–0593. doi:10.5539/jmsr.v5n2p100
20. Zuperl U, Cus F (2003) Optimization of cutting conditions during cutting by using neural networks. *Robot Comput Integr Manuf* 19(1–2):189–199. doi:10.1016/S0736-5845(02)00079-0
21. Senthilkumaar JS, Selvarani P, Arunachalam RM (2012) Intelligent optimization and selection of machining parameters in finish turning and facing of Inconel 718. *Int J Adv Manuf Technol* 58(9–12): 885–894. doi:10.1007/s00170-011-3455-7
22. Zinati RF, Razfar MR (2012) Constrained optimum surface roughness prediction in turning of X20Cr13 by coupling novel modified harmony search-based neural network and modified harmony search algorithm. *Int J Adv Manuf Technol* 58(1–4):93–107. doi:10.1007/s00170-011-3393-4
23. Jafarian F, Taghipour M, Amirabadi H (2013) Application of artificial neural network and optimization algorithms for optimizing surface roughness, tool life and cutting forces in turning operation. *J Mech Sci Technol* 27(5):1469–1477. doi:10.1007/s12206-013-0327-0
24. Mokhtari Homami R, Fadaei Tehrani A, Mirzadeh H, Movahedi B, Azimifar F (2014) Optimization of turning process using artificial intelligence technology. *Int J Adv Manuf Technol* 70(5–8):1205–1217. doi:10.1007/s00170-013-5361-7
25. Tamang SK, Chandrasekaran M. (2015) Modeling and optimization of parameters for minimizing surface roughness and tool wear in turning Al/SiCp MMC, using conventional and soft computing techniques. *Advances in Production Engineering And Management* 10(2):59–72. Doi:10.14743/apem2015.2.192
26. Sangwan KS, Saxena S, Kant G (2015) Optimization of machining parameters to minimize surface roughness using integrated ANN-GA approach. *Procedia CIRP* 29:305–310. doi:10.1016/j.procir.2015.02.002
27. Gupta AK, Guntuku SC, Desu RK, Balu A (2015) Optimisation of turning parameters by integrating genetic algorithm with support vector regression and artificial neural networks. *Int J Adv Manuf Technol* 77(1–4):331–339. doi:10.1007/s00170-014-6282-9
28. Basak S, Dixit US, Davim JP (2007) Application of radial basis function neural networks in optimization of hard turning of AISI D2 cold-worked tool steel with a ceramic tool. *Proc Inst Mech Eng B J Eng Manuf* 221(6):987–998. doi:10.1243/09544054JEM737
29. Karpat Y, Özel T (2007) Multi-objective optimization for turning processes using neural network modeling and dynamic-neighborhood particle swarm optimization. *Int J Adv Manuf Technol* 35(3–4):234–247. doi:10.1007/s00170-006-0719-8
30. Yue C, Wang L, Liu J, Hao S (2016) Multi-objective optimization of machined surface integrity for hard turning process. *Int J Smart Home* 10(6):71–76. doi:10.14257/ijsh.2016.10.6.08
31. Abbas AT, Hamza K, Aly MF, Al-Bahkali EA (2016) Multiobjective optimization of turning cutting parameters for j-steel material. *Mater Sci Eng* 6429160:8. doi:10.1155/2016/6429160
32. Feng C-XJ YZ-GS, Kingi U, Pervaiz BM (2005) Threefold vs. fivefold cross validation in one-hidden-layer and two-hidden-layer predictive neural network modeling of machining surface roughness data. *J Manuf Syst* 24(2):93–107. doi:10.1016/S0278-6125(05)80010-X
33. Feng C-XJ YZ-GS, Emanuel JT, Li P-G, Shao X-Y, Wang Z-H (2008) Threefold versus fivefold cross-validation and individual versus average data in predictive regression modelling of machining experimental data. *Int J Comput Integ Manuf* 21(6):702–714. doi:10.1080/09511920701530943
34. Asiltürk I, Kahramanli H, El Mounayri H (2012) Prediction of cutting forces and surface roughness using artificial neural network (ANN) and support vector regression (SVR) in turning 4140 steel. *Mater Sci Technol* 28(8):980–986. doi:10.1179/1743284712Y.00000000043
35. Statnikov RB, Matusov J (1996) Use of Pt-nets for the approximation of the Edgeworth-Pareto set in multicriteria optimization. *J Optim Theory Appl* 91(3):543–560
36. Berezkin VE, Lotov AV (2014) Comparison of two Pareto frontier approximations. *Comp Math Math Phys* 54(9):1402–1410. doi:10.1134/S0965542514090048

37. Lotov AV, Ryabikov AI, Buber AL (2014) Pareto frontier visualization in the development of release rules for hydro-electrical power stations. *Sci Tech Inf Process* 41(5):314–324. doi:[10.3103/S0147688214050025](https://doi.org/10.3103/S0147688214050025)
38. Carvalho M, Ambrósio J, Eberhard P (2011) Identification of validated multibody vehicle models for crash analysis using a hybrid optimization procedure. *Struct Multidisc Optim* 44(1):85–97. doi:[10.1007/s00158-010-0590-y](https://doi.org/10.1007/s00158-010-0590-y)
39. Choudhary AK, Harding JA, Tiwari MK (2009) Data mining in manufacturing: a review based on the kind of knowledge. *J Intell Manuf* 20(5):501–521. doi:[10.1007/s10845-008-0145-x](https://doi.org/10.1007/s10845-008-0145-x)
40. Wang X, Feng CX (2002) Development of empirical models for surface roughness prediction in finish turning. *Int J Adv Manuf Technol* 20(5):348–356. doi:[10.1007/s001700200162](https://doi.org/10.1007/s001700200162)
41. Al-Ahmari AMA (2007) Predictive machinability models for a selected hard material in turning operations. *J Mater Process Technol* 190(1–3):305–311. doi:[10.1016/j.jmatprotec.2007.02.031](https://doi.org/10.1016/j.jmatprotec.2007.02.031)
42. Jack Feng C-X, Yu Z-GS, Kingi U, Pervaiz BM (2005) Threefold vs. fivefold cross validation in one-hidden-layer and two-hidden-layer predictive neural network modeling of machining surface roughness data. *J Manuf Syst* 24(2):93–107. doi:[10.1016/S0278-6125\(05\)80010-X](https://doi.org/10.1016/S0278-6125(05)80010-X)
43. Nogin VD. Decision making in multicriteria environment: quantitative approach. M.: FIZMATLIT, 2002, P.144. **[in Russian]**
44. Kostenetskiy PS, Safonov AY (2016) SUSU supercomputer resources. *CEUR Workshop Proceedings* 1576:561–573